Accelerated Exchange of a Buried Water Molecule in Selectively Disulfide-Reduced Bovine Pancreatic Trypsin Inhibitor†

Vladimir P. Denisov,‡ Jörg Peters,§ Hans Dietrich Hörlein,§ and Bertil Halle*,‡

Department of Biophysical Chemistry, Lund University, P.O. Box 124, SE-22100 Lund, Sweden, and Bayer HealthCare AG, Pharma Operations Biotechnology, Friedrich-Ebert Strasse 217, D-42096 Wuppertal, Germany

Received April 21, 2004; Revised Manuscript Received June 7, 2004

ABSTRACT: Using magnetic relaxation dispersion (MRD), we have previously shown that the four internal water molecules in bovine pancreatic trypsin inhibitor (BPTI) exchange with bulk water on time scales between 10^{-8} and 10^{-4} s at room temperature. Because this exchange is controlled by the protein structure, internal water molecules can be used to probe rare conformational fluctuations. Here, we report ^{2}H and ^{17}O MRD data at three temperatures for wild-type BPTI and two BPTI variants where the 14−38 disulfide bond has been cleaved by a double Cys → Ser mutation or by disulfide reduction and carboxamidomethylation. The MRD data show that the internal water molecules are conserved on disulfide cleavage. However, the exchange rate of the water molecule buried near the disulfide bond is enhanced by 2−4 orders of magnitude. The relation of water exchange to other dynamic processes in BPTI is discussed.

The exceptional stability of bovine pancreatic trypsin inhibitor (BPTI)[1] with respect to heat and solvent denaturation is largely due to three disulfide bonds, which lower the conformational entropy of unfolded conformers (*1*). If all three disulfides are reduced, BPTI unfolds even under physiological conditions. The oxidative folding pathway of fully reduced BPTI involves several intermediates with nonnative disulfide pairings and has been elucidated in great detail (*2*, *3*). Two of the disulfide bonds (5−55 and 30−51) in BPTI are completely buried in the hydrophobic core, but the third one (14−38) is located on the protein surface with about 50% solvent exposure of the sulfur atoms. The 14−38 disulfide bridges two extensive loops, comprising residues 8−17 and 36−44 (*4*), that contain most of the primary, 13−18, and secondary, 34−39, proteinase binding loops responsible for the extremely tight association ($K_a \approx 10^{13}$ M^{-1}) of BPTI with bovine β-trypsin (*5*). The rigidity of these loops is thought to be essential for the inhibitory function of BPTI (*6*). While the backbones of the two loops are connected by only two intramolecular hydrogen bonds (16 N−36 O and 36 N−11 O), additional stabilization is provided by buried water molecules.

All reported crystal structures of wild-type BPTI (*7*−*9*) locate four water molecules in the deep groove between the two loops (Figure 1). These four internal water molecules, labeled W111, W112, W113, and W122, are extensively

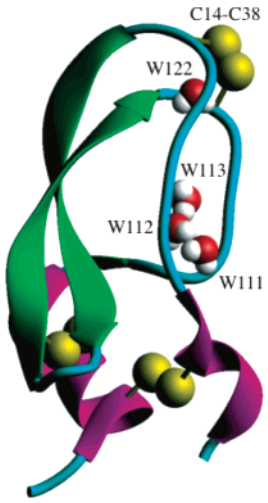

FIGURE 1: Location of the internal water molecules (W111, W112, W113, and W122) and the three disulfide bonds in the crystal structure of BPTI (*4*).

hydrogen bonded to the protein, forming an integral part of the native BPTI molecule. Altogether, they are involved in 13 hydrogen bonds with the protein by with each other, bridging the backbones of the two loops in four places: Tyr10 N−W112−Asn43 O, Lys41 N−W113−Tyr10 O, Cys14 N−W122−Cys38 O, and Cys38 N−W122−Thr11 O. These four water molecules should therefore be present at the same locations also in solution (*7*), an expectation that has subsequently been confirmed by several NMR relaxation studies (*10*−*13*). Although they can be considered as an extension of the protein structure, all four internal water molecules exchange with bulk water on the nanosecond to millisecond time scale. The three mutually hydrogen-bonded internal water molecules W111−W113 have mean residence times in the range 10^{-8}−10^{-6} s at 27 °C (*12*). The singly buried W122 exchanges more slowly, with a residence time

† This work was supported by the Swedish Research Council.

* To whom correspondence should be addressed. Fax: 46-46-2224543. Tel: 46-46-2229516. E-mail: bertil.halle@bpc.lu.se.

‡ Lund University.

§ Bayer HealthCare AG.

[1] Abbreviations: BPTI, bovine pancreatic trypsin inhibitor; BPTI-CS, BPTI double mutant C14S/C38S; BPTI-RCAM, BPTI variant where the 14−38 disulfide bond has been cleaved by selectively reducing and carboxamidomethylating C14 and C38; BPTI-R and BPTI-RM, 14−38 reduced BPTI variants with free thiols and methylated thiols, respectively; CD, circular dichroism; MRD, magnetic relaxation dispersion.

10.1021/bi0492049 CCC: $27.50
Published on Web 08/28/2004

of 170 ± 20 μs at 27 °C (*13*), presumably because of the nearby 14−38 disulfide bond.

In the present work, we assess the role of the 14−38 disulfide bond in maintaining the native protein structure and in suppressing conformational fluctuations. Specifically, we examine the effect of cleaving the 14−38 disulfide on the integrity and exchange kinetics of the internal water molecules. To this end, we use water ^{2}H and ^{17}O MRD measurements to probe the internal water molecules in wild-type BPTI and in two BPTI variants where the 14−38 disulfide bond has been cleaved either by the double mutation C14S/C38S or by selectively reducing and carboxamidomethylating C14 and C38. We refer to these BPTI variants as BPTI-CS and BPTI-RCAM, respectively.

Because of its exposed location, the 14−38 disulfide bond can be selectively reduced while leaving the other two disulfide bonds intact (*14*, *15*). To prevent reoxidation, the free thiols are often blocked, e.g., by methylation or carboxamidomethylation (*16*). In the following, we refer to 14−38 reduced BPTI variants with free thiols or with methylated thiols as BPTI-R and BPTI-RM, respectively. Although cleavage of the 14−38 disulfide reduces the stability of BPTI toward heat and solvent denaturation (*17*−*20*), BPTI-R and BPTI-RCAM are still capable of inhibiting β-trypsin as long as proteolysis does not interfere (*14*, *16*). Several studies of the folding pathway of BPTI have employed mutants lacking the 14−38 disulfide bond, specifically C14A/C38A (*21*−*24*), C14T/C38T (*21*), and C14S/C38S (*25*), which all appear to be very similar to the reduced and alkylated variants, such as BPTI-RM and BPTI-RCAM.

MATERIALS AND METHODS

Materials. The BPTI mutant Met(−1)-C14S/C38S (BPTI-CS) was prepared according to the procedure described for the G36S and Y35G mutants (*26*, *27*). The purified (96%) protein was lyophilized as a salt of trifluoroacetic acid. Both the BPTI-CS mutant and wild-type BPTI (bovine aprotinin; Trasylol) were desalted by extensive dialysis against pure water, followed by lyophilization.

BPTI with the 14−38 disulfide bond selectively reduced and carboxamidomethylated (BPTI-RCAM) was prepared according to procedures described in the literature (*21*, *28*, *29*). The lyophilized protein was quickly dissolved (at 185 μM) in 0.1 M Tris-HCl buffer (pH 8.7), 1 mM EDTA, and 10 mM reduced dithiothreitol (>97%; Wako) and incubated for 24 min at room temperature. The reaction was quenched by shifting the pH to ca. 1.5 by addition of formic acid to 16% v/v. The solution was dialyzed against 5% formic acid (pH 1.5−1.7) and 1 mM EDTA and lyophilized. To block the free thiols, the protein powder was dissolved (at 5.5 mM) in 10 mM HCl and then diluted 10-fold with a solution of 0.1 M Tris-HCl (pH 8.7), 1 mM EDTA, and 10 mM iodoacetamide (Sigma). The reaction was quenched after 30 min of incubation at room temperature in the dark by adding formic acid to 28% v/v. The solution was again dialyzed against 1% formic acid and pure water and then lyophilized.

The concentration of free thiols in the selectively reduced protein before and after blocking with iodoacetamide was checked by reaction with Ellman's reagent (*30*) and 5,5′-dithiobis(2-nitrobenzoic acid) (DTNB, 99%; Aldrich). The absorbance at 412 nm of ca. 10 μM protein solutions in 0.1 M phosphate buffer (pH 7.3) and 1 mM EDTA was measured before and after addition of 10 μL/mL freshly prepared 15 mM DTNB (in the same buffer). The difference was corrected by the absorbance of the same amount of DTNB in the pure buffer. The concentration of free thiols was calculated using an apparent extinction coefficient for the 2-nitro-5-thiobenzoate anion of 13.9 mM^{-1} cm^{-1}. The latter was obtained from a separate assay with cysteine (>98%; Sigma) and reduced dithiothreitol, with concentrations calculated on the basis of dry weight. This procedure yielded a free thiol concentration (in moles of SH per mole of protein) of 2.1 ± 0.1 before and 0.003 ± 0.003 after blocking the protein with iodoacetamide.

Protein solutions for MRD measurements were made by dissolving the lyophilized protein in a 50:50% w/w mixture of D_2O and H_2O enriched to 35% in ^{17}O (both from Cambridge Isotope Laboratories). No buffer was used. The pH value (without correction for isotope effects) was adjusted to 5.2 by adding small amounts of concentrated HCl. The BPTI-RCAM solution was centrifuged several times to remove a small fraction of aggregated protein, whereafter the sample remained clear for several months. The absorbance at 280 nm of wild-type BPTI, BPTI-CS, and BPTI-RCAM samples was 73.0 ± 2.0, 72.8 ± 2.0, and 72.8 ± 2.0, respectively. Protein concentrations of wild-type and mutant proteins in the MRD samples were determined by complete amino acid analysis, yielding 13.4 ± 0.3 mM for both. This corresponds to a water/protein mole ratio N_T = 3870 ± 80.

Relaxation Dispersion Measurements. The longitudinal relaxation rates, $R_1(\omega_0)$, of the water ^{2}H and ^{17}O resonances were measured as described previously (*11*, *31*) at 10 magnetic fields in the range 0.38−14.1 T using five Bruker and Varian NMR spectrometers with four fixed-field cryomagnets and a field-variable iron magnet. The sample temperature was maintained within ±0.1 °C of the target value (4, 27, or 55 °C) by a thermostated air flow. The ^{2}H and ^{17}O relaxation rates, R_{bulk}, of a bulk water reference sample, with the same solvent isotope composition as in the protein solutions, were also measured at each temperature.

The MRD profiles were modeled with a single correlation time according to (*32*)

$$R_1(\omega_0) = R_{bulk} + \alpha + \beta\tau_c\left[\frac{0.2}{1+(\omega_0\tau_c)^2} + \frac{0.8}{1+(2\omega_0\tau_c)^2}\right] \quad (1)$$

where ω_0 is the variable (angular) resonance frequency. The high-frequency relaxation excess, $\alpha = R_1(\omega_0 \gg 1/\tau_c) - R_{bulk}$, represents the contribution from mobile water molecules at the protein surface and can be expressed as (*32*)

$$\alpha = \frac{N_S}{N_T} R_{bulk}\left(\frac{\tau_S}{\tau_{bulk}} - 1\right) \quad (2)$$

where N_S is the number of water molecules in contact with the protein surface, estimated as 268 for BPTI (*33*), τ_S the average of the (local) rotational correlation time of these water molecules, and τ_{bulk} the rotational correlation time of bulk water. The ratio τ_S/τ_{bulk} is known as the rotational retardation factor.

The dispersion amplitude parameter, β, is given by (*32*)

$$\beta = \frac{N_I}{N_T}(\omega_Q S_I)^2 \quad (3)$$

where N_I is the number of long-lived internal water molecules in the protein, S_I is their (root-mean-square) orientational order parameter, and ω_Q is the water ^2H or ^{17}O rigid-lattice nuclear quadrupole frequency. Since the ice Ih quadrupole frequencies used here ($\omega_Q = 7.61 \times 10^6$ rad s^{-1} for ^{17}O and 8.70×10^5 rad s^{-1} for ^2H) incorporate the asymmetry parameter of the electric field gradient tensor and are corrected for librational averaging (*27*), the order parameter S_I has a maximum value of unity for both ^{17}O and ^2H ($S_I = 0.94$ for water molecules in ice Ih).

The molecular interpretation of the correlation time, τ_c, and the dispersion amplitude, β, depends on the relative time scales of molecular exchange and nuclear spin relaxation of the internal water molecules. The time scale for exchange of an internal water molecule with bulk water is characterized by the mean residence time, τ_W, in the internal hydration site. In the so-called fast-exchange limit, τ_W is short compared to the intrinsic spin relaxation time, T_I, of the internal water molecule. Because T_I increases monotonically with the resonance frequency, ω_0, the dispersion profile can be analyzed in the fast-exchange limit only if $\tau_W \ll T_I(0)$, where the zero-frequency intrinsic spin relaxation rate is given by $T_I(0) = (\omega_Q^2 S_I^2 \tau_c)^{-1}$.

An internal water molecule may contribute significantly to the dispersion profile even if it is not fully in the fast-exchange limit. The resulting dispersion profile can still be described by eq 1, but the parameters β (or N_I) and τ_c must then be regarded as apparent quantities, related to the molecular parameters β and τ_c through (*32*)

$$N_I^{app} = N_I[1 + (\omega_Q S_I)^2 \tau_c \tau_W]^{-1/2} \quad (4)$$

and

$$\tau_c^{app} = \tau_c[1 + (\omega_Q S_I)^2 \tau_c \tau_W]^{-1/2} \quad (5)$$

In the fast-exchange limit, where $\tau_W \ll (\omega_Q^2 S_I^2 \tau_c)^{-1}$, these expressions reduce to $N_I^{app} = N_I$ and $\tau_c^{app} = \tau_c$. In the opposite, slow-exchange, limit, where $\tau_W \gg (\omega_Q^2 S_I^2 \tau_c)^{-1}$, the internal water molecule does not contribute significantly to the observed dispersion ($N_I^{app} \ll N_I$) since the relaxation of the internal and bulk water magnetizations are dynamically decoupled. (The transition from the fast-exchange to the slow-exchange limit is graphically illustrated in Figure 3 of ref *13*.)

The correlation time, τ_c, measures how quickly an internal water molecule loses "memory" of its orientation (with respect to the external magnetic field). This orientational randomization can occur by either of two processes: by rotational diffusion of the protein, with rotational correlation time τ_R, or by transfer to the bulk solvent, where a water molecule rotates 3 or more orders of magnitude faster than τ_R. Because these two processes are independent, their rates are additive (*32*): $1/\tau_c = 1/\tau_R + 1/\tau_W$. On the basis of previous studies of BPTI (*11*−*13*), we assume that $\tau_W \gg \tau_R$ for the internal water molecules responsible for the dispersion. We can then set $\tau_c = \tau_R$ in eqs 1, 4, and 5.

The MRD data are reasonably well described at all temperatures by a dispersion function with a single correlation time, τ_c, as in eq 1. However, in nearly all cases small systematic deviations are evident, and fits of significantly higher quality can be obtained by invoking two correlation times. The observed deviations from a Lorentzian (single correlation time) dispersion law are indeed expected on several grounds. First, over the temperature range examined here, the most long-lived of the internal water molecules in wild-type BPTI, W122, is in fast to intermediate exchange for ^2H and slow to intermediate exchange for ^{17}O (*13*). When an internal water molecule makes a significant contribution to the dispersion without being fully in the fast-exchange limit, the effective correlation time, τ_c, will be shorter than the rotational correlation time, τ_R, of the protein (see eq 5). Second, at the protein concentration used here, we expect that a few percent of the BPTI molecules self-associate into decamers (*34*). [Because the 14−38 disulfide bond is on the exposed outer surface of the decamer (*35*), its cleavage should not significantly affect the monomer−decamer equilibrium.] Despite their small population, the decamers contribute significantly to the low-frequency part of the dispersion profile since their rotational correlation time is 8 times longer than for the monomer (*34*). Third, labile BPTI hydrogens contribute to the ^2H dispersion at 55 °C with effective correlation times that depend on the hydrogen exchange rates. Finally, a few partially buried water molecules in surface pockets (possibly including W111) may, depending on the temperature, have residence times longer than 1 ns but not much longer than τ_R. They will then contribute to the high-frequency part of the dispersion.

Although the increase from three to five adjustable parameters is justified by the statistical *F* test, the resulting parameters have large covariances and are sensitive to small measurement errors. To obtain robust results, it is then necessary to hold at least one correlation time fixed during the fit. However, because of the several temperature-dependent intermediate-exchange and self-association effects, the correlation times cannot be predicted with useful accuracy. With MRD data extending over less than 2 decades, we must therefore resort to single correlation time fits. Because fits with one or two (fixed or adjustable) correlation times yield similar values for the total dispersion amplitude β, or the derived quantity $N_I^{app} S_I^2$, we believe that these parameters are robust, even if the accuracy is somewhat lower than the quoted precision. The apparent correlation time, τ_c, derived from the fits is affected by the aforementioned complications, but it is not essential for our analysis.

Circular Dichroism Measurements. CD measurements on ca. 0.2 mM solutions of BPTI-CS or BPTI-RCAM in H_2O at pH 4.6 were performed with a JASCO J-720 spectropolarimeter, equipped with a PTC-343 Peltier-type variable-temperature cell. Temperature scans at 275 nm were performed between 25 and 90 °C with a resolution of 1 °C. The thermal denaturation curves resulting from averaging of the forward and reverse scans were fitted using a two-state (single-transition) model. Since the high-temperature slope of the curves could not be accurately estimated from the data, it was set to zero in the fits.

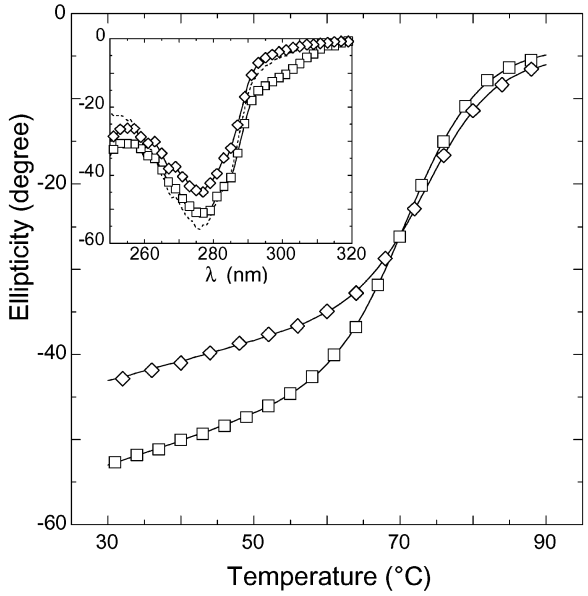

FIGURE 2: CD temperature scans at 275 nm from 0.2 mM solutions of BPTI-CS (squares) and BPTI-RCAM (diamonds). The curves resulted from fits based on a two-state model. The insert shows spectra in the near-UV range at room temperature, with the wild-type BPTI spectrum (dashed) as a reference.

RESULTS

Thermal Stability of BPTI Disulfide Variants. The near-UV CD spectra of BPTI-CS and BPTI-RCAM (Figure 2, insert) demonstrate that the tertiary structure is intact in the selectively reduced BPTI variants. The small deviations from the spectrum of wild-type BPTI can be attributed to the modified 14−38 disulfide bond and to the nearby Tyr35 (*36*). The temperature scans at 275 nm (Figure 2) are characteristic of a single (two-state) transition, with nearly complete denaturation at 90 °C.

From the CD data in Figure 2, we obtained denaturation midpoint temperatures, T_m, of 71.8 ± 0.1 °C for BPTI-CS and 74.5 ± 0.1 °C for BPTI-RCAM, about 20−25 °C below T_m for wild-type BPTI. Our T_m value for BPTI-RCAM is consistent with the previously reported value of 76 °C for this variant in D_2O at pH 5.3 (*37*). In the BPTI-CS mutant, the disulfide bond is presumably replaced by a hydrogen bond between the hydroxyl groups of S14 and S38. In BPTI-RCAM, the asparagyl group attached to each of the sulfur atoms can also form a hydrogen bond.

MRD Profiles. Figure 3 shows the ^{17}O and ^{2}H MRD profiles from 13.4 mM solutions of wild-type BPTI, BPTI-CS, and BPTI-RCAM at pH 5.2. For each BPTI variant, MRD measurements were carried out at three temperatures: 4, 27, and 55 °C. According to the CD data in Figure 2, less than 2% and 3% of BPTI-RCAM and BPTI-CS, respectively, is in the denatured state at 55 °C. Therefore, the MRD data refer to the native (fully folded) forms of the three BPTI variants. The dispersions observed in the frequency range 1−100 MHz are produced by the internal water molecules in BPTI. At pH 5.2, the contribution to the ^{2}H dispersion from labile BPTI hydrogens is negligibly small at 4 and 27 °C (*31*) but not at 55 °C (see below). The MRD data are reasonably well described at all temperatures by a dispersion function with a single correlation time, τ_c, as in eq 1. The values of the three parameters, τ_S/τ_{bulk}, $N_I^{app}S_I^2$, and τ_c, obtained from fits to each profile, as described in Materials and Methods, are collected in Table 1.

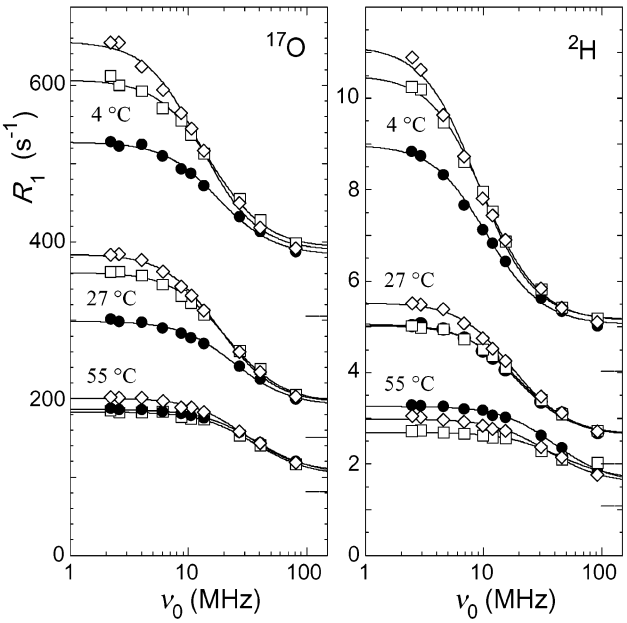

FIGURE 3: Dispersion of the water ^{17}O (left) and ^{2}H (right) longitudinal relaxation rate in aqueous solutions of wild-type BPTI (circles), BPTI-CS (squares), and BPTI-RCAM (diamonds) at 4, 27, and 55 °C. The estimated error bars are comparable to the size of the data symbols. The curves resulted from Lorentzian fits according to eq 1. For each temperature, the bulk relaxation rate, R_{bulk}, is indicated by a line segment on the right.

Table 1: Results of Single Correlation Time Fits to ^{2}H and ^{17}O MRD Data from Wild-Type BPTI, BPTI-CS, and BPTI-RCAM at pH 5.2[a]

BPTI	nucleus	T (°C)	τ_S/τ_{bulk}	$N_I^{app}S_I^2$	τ_c (ns)	R_{bulk} (s^{-1})
wild type	^{17}O	4	4.7(1)	1.9(1)	5.1(2)	305(3)
CS	^{17}O	4	5.2(1)	2.5(1)	5.8(2)	
RCAM	^{17}O	4	5.0(1)	2.5(1)	7.1(2)	
wild type	^{17}O	27	4.9(1)	1.9(1)	3.7(1)	151(2)
CS	^{17}O	27	5.3(1)	2.6(1)	4.3(1)	
RCAM	^{17}O	27	5.2(1)	2.6(1)	5.0(1)	
wild type	^{17}O	55	5.1(2)	2.3(1)	2.4(1)	81.2(8)
CS	^{17}O	55	4.7(2)	2.2(2)	2.5(1)	
RCAM	^{17}O	55	5.6(2)	2.1(1)	3.0(1)	
wild type	^{2}H	4	4.7(1)	2.4(1)	8.5(2)	4.03(4)
CS	^{2}H	4	5.0(1)	3.1(1)	8.8(1)	
RCAM	^{2}H	4	5.0(1)	3.0(1)	10.1(1)	
wild type	^{2}H	27	5.4(1)	2.6(1)	4.7(1)	2.01(2)
CS	^{2}H	27	5.4(1)	2.7(1)	4.5(1)	
RCAM	^{2}H	27	5.6(1)	2.9(1)	5.1(1)	
wild type	^{2}H	55	6.5(3)	3.8(1)	2.2(1)	1.09(1)
CS	^{2}H	55	8.6(7)	1.9(2)	2.6(2)	
RCAM	^{2}H	55	7.5(2)	2.8(1)	2.6(1)	

[a] Numbers within parentheses are parameter errors (one standard deviation) in the last position, obtained by the Monte Carlo method using 1000 synthetic data sets.

The high-frequency plateau of the dispersion profile is only affected by mobile water molecules at the protein surface. The relaxation excess, $R_1 - R_{bulk}$, at the plateau provides information about the average rotational correlation time, τ_S, of all water molecules interacting with the external surface of the protein. This parameter is usually expressed relative to the bulk water rotational correlation time, τ_{bulk}, as the so-called rotational retardation factor, τ_S/τ_{bulk}. The near convergence at high frequencies of the three MRD profiles at each temperature (Figure 3), and the similar values

of τ_S/τ_{bulk} obtained from the fits (Table 1), demonstrates that the surface hydration is virtually the same for BPTI-CS and BPTI-RCAM as for wild-type BPTI. This observation is consistent with previous studies, showing that cleavage of the 14−38 disulfide bond (and blocking of the free thiols) only affects the protein structure locally (*17*, *29*, *37*−*40*). At 4 and 27 °C, the ^{2}H and ^{17}O data yield the same rotational retardation factor, as expected for nearly isotropic water dynamics in the hydration layer (*32*). The larger τ_S/τ_{bulk} values derived from the ^{2}H data at 55 °C indicate that about one-third of the high-frequency relaxation excess is contributed by labile BPTI hydrogens in fast or intermediate exchange with water hydrogens at this temperature. Excluding the 55 °C ^{2}H data, we find no significant temperature dependence in τ_S/τ_{bulk}, and the average over the 15 data sets is 5.1, in agreement with the previously determined value of 5.5 ± 0.4 for BPTI (*11*, *33*) and the mean value of 5.4 ± 0.6 for 11 proteins (*41*).

The effective correlation time, τ_c, obtained from the Lorentzian fits in Figure 3 may be compared to the expected rotational correlation time, τ_R, of monomeric BPTI. The best available estimate of τ_R comes from a ^{15}N relaxation study of 3 mM BPTI (at this low concentration the decamer population is negligible) in 10% D_2O, pH 4.7, and 25 °C (*42*). Assuming that τ_R is proportional to η/T and scaling the ^{15}N result to the viscosity of our isotope-enriched water, we obtain τ_R = 7.6, 3.6, and 1.9 ns at 4, 27, and 55 °C, respectively. The modest deviations of the effective τ_c in Table 1 from these τ_R values can be attributed to self-association of a small fraction of the BPTI molecules and to variations in the effective correlation time of the several long-lived water molecules responsible for the dispersion (see Materials and Methods). With its smaller quadrupole frequency, ω_Q, the ^{2}H isotope is more sensitive to self-association and therefore yields longer τ_c values. The BPTI-CS mutant yields essentially the same τ_c as wild-type BPTI, despite the additional N-terminal methionine residue in the mutant. The slightly longer τ_c for the BPTI-RCAM variant may be a direct effect of the blocking groups on the protein rotational friction or an indirect effect of these groups on protein−protein interactions and self-association (see Materials and Methods).

Internal Water Molecules. The focus of this work is on the parameter $N_I^{app}S_I^2$, the product of the apparent number of long-lived water molecules and their mean-square orientational order parameter. Here, "long-lived" means that the water residence time, τ_W, is longer than about 1 ns. Previous MRD studies have established that the only long-lived water molecules in BPTI at the temperatures investigated here are the four internal water molecules (*11*−*13*). If the residence time is sufficiently long, the fast-exchange condition $(\omega_Q S_I)^2\tau_R\tau_W \ll 1$ is violated. As shown by eq 4, N_I^{app} will then be smaller than the actual number, N_I, of long-lived water molecules.

The excess ^{2}H relaxation at high frequencies (and the derived parameter τ_S/τ_{bulk}) indicates a significant contribution from labile BPTI hydrogens at 55 °C. The large ^{2}H dispersion amplitude at 55 °C, corresponding to $N_I^{app}S_I^2$ = 3.8 (Table 1), also suggests a labile hydrogen contribution. (The smaller $N_I^{app}S_I^2$ values for the disulfide-cleaved variants might be explained by fast 180° flips at 55 °C of internal water molecules.) Because we cannot separate the water and labile hydrogen contributions, we exclude the 55 °C ^{2}H data from the following analysis.

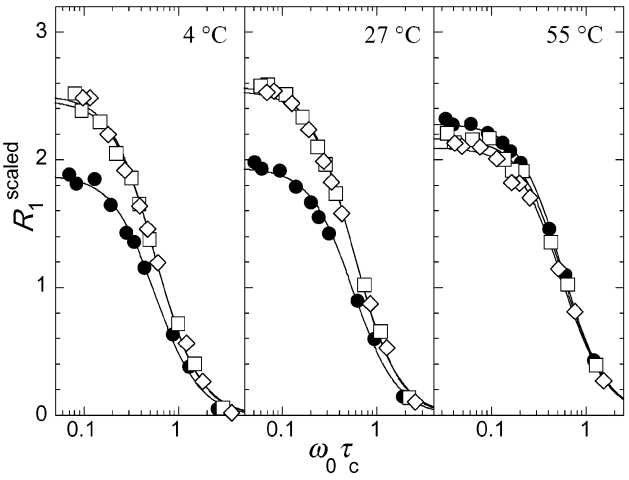

FIGURE 4: Same ^{17}O MRD data as in Figure 3 but scaled according to $R_1^{scaled} = (R_1 - R_{bulk} - \alpha)N_T/(\omega_Q^2\tau_c)$ and presented separately for 4 °C (left), 27 °C (middle), and 55 °C (right). The curves were scaled in the same way as the corresponding data points. The symbols refer to wild-type BPTI (circles), BPTI-CS (squares), and BPTI-RCAM (diamonds).

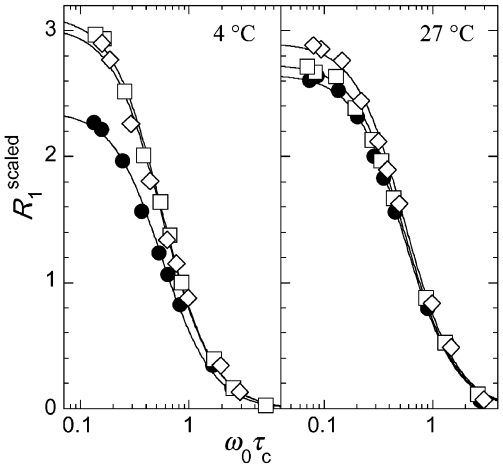

FIGURE 5: Same ^{2}H MRD data as in Figure 3 but scaled as in Figure 4.

To visualize differences in $N_I^{app}S_I^2$ among the BPTI variants, it is helpful to scale the relaxation rates according to $R_1^{scaled} = (R_1 - R_{bulk} - \alpha)N_T/(\omega_Q^2\tau_c)$ (*12*, *27*). According to eqs 1 and 3, the low-frequency limit of the scaled dispersion profile directly yields the quantity $N_I^{app}S_I^2$. In Figures 4 and 5, the scaled ^{17}O and ^{2}H dispersion profiles are plotted against the dimensionless frequency variable $\omega_0\tau_c$ to remove the effect of the slight variation in the correlation time τ_c.

Referring to Table 1 and Figures 4 and 5, we note that, at all temperatures and for both nuclei (except at 55 °C for ^{2}H, where labile hydrogens contribute), $N_I^{app}S_I^2$ has the same value (within the error bounds) for BPTI-CS and BPTI-RCAM. From the ^{17}O data, we obtain $N_I^{app}S_I^2(^{17}O) = 2.5 \pm 0.2$ for the two BPTI variants lacking the 14−38 disulfide bond. The temperature dependence of $N_I^{app}S_I^2(^{17}O)$ is weak or insignificant (at the two lower temperatures). Because τ_W is expected to be strongly temperature-dependent, this means that the contributing water molecules are in the fast-exchange

limit, with $\tau_W \ll (\omega_Q S_I)^{-2}\tau_R^{-1} \approx 1\ \mu$s at 27 °C. The ^{2}H data yield a slightly larger value, $N_I^{app}S_I^2(^2H) = 2.9 \pm 0.2$, in agreement with our previous studies of wild-type BPTI and mutants (*11*, *12*, *31*). This ca. 30% difference between $N_I^{app}S_I^2(^2H)$ and $N_I^{app}S_I^2(^{17}O)$ has previously been attributed to twist librations of water molecules W111−113 of about 20° amplitude (*12*, *27*), which reduce $S_I(^{17}O)$ more than $S_I(^2H)$. A water molecule with a residence time in the range $10^{-6}-10^{-4}$ s would only contribute to $N_I^{app}S_I^2(^2H)$, but then we would also expect a temperature dependence (according to eq 4) in $N_I^{app}S_I^2(^{17}O)$, whereas no significant temperature dependence in $N_I^{app}S_I^2$ is observed for either nucleus.

For wild-type BPTI, not only is $N_I^{app}S_I^2(^2H)$ significantly larger than $N_I^{app}S_I^2(^{17}O)$, but both $N_I^{app}S_I^2(^{17}O)$ and $N_I^{app}S_I^2(^2H)$ increase with temperature. These findings are consistent with a previous temperature-dependent MRD study (*13*), where they were attributed to intermediate-exchange effects (according to eq 4) on the contribution from the most slowly exchanging internal water molecule, W122, with a residence time of 170 ± 20 μs at 27 °C. According to that study, W122 should contribute 0.02 (4 °C), 0.14 (27 °C), and 0.63 (55 °C) to $N_I^{app}S_I^2(^{17}O)$ and 0.18 (4 °C) and 0.72 (27 °C) to $N_I^{app}S_I^2(^2H)$. These values are derived from fits to difference-MRD profiles where R_1 for the G36S mutant lacking W122 was subtracted from R_1 for wild-type BPTI. Such difference-MRD fits were not perfomed here, because the effective correlation time of W122 is different in wild-type and disulfide-cleaved BPTI. Since the MRD data exhibit small but systematic deviations from single-Lorentzian dispersion shape (see Materials and Methods), the two types of single-Lorentzian fit are not expected to yield identical results. The lack of quantitative agreement between the present (Table 1) and previous (*13*) results can thus be largely attributed to the single-Lorentzian approximation. Nevertheless, the semiquantitative agreement leaves little doubt that we are observing the same transition from slow to fast exchange of W122 as in the previous study. In other words, the residence time of W122 becomes shorter with increasing temperature, so that the fast exchange condition, $\tau_W \gg T_1$ (see Materials and Methods), is satisfied at higher temperatures.

The salient feature of Table 1 and Figures 4 and 5 is the finding that $N_I^{app}S_I^2$ for the disulfide-cleaved variants is significantly larger than for wild-type BPTI at temperatures where W122 is expected to make only a small contribution to $N_I^{app}S_I^2$ for wild-type BPTI. On the other hand, at temperatures where W122 is known to contribute substantially for wild-type BPTI, the dispersion profiles differ little among the three BPTI variants. This behavior is evident for ^{17}O at 55 °C (Figure 4) and for ^{2}H at 27 °C (Figure 5). On the basis of these observations, we conclude that the internal water molecules in wild-type BPTI are also present in the disulfide-cleaved variants. Moreover, the results indicate that cleavage of the 14−38 disulfide bond accelerates the exchange of W122 by several orders of magnitude. At 27 °C, cleavage of the disulfide bond thus decreases the residence time of W122 from 170 to ≪1 μs. Consistent with this scenario, we find that the difference $N_I^{app}S_I^2$(CS/RCAM) − $N_I^{app}S_I^2$(wild-type) decreases with increasing temperature for both nuclei.

DISCUSSION

Cleavage of a disulfide bond affects a protein in several ways. The most obvious effect is a local relaxation to a different conformational "ground state". Removal of the topological constraint also alters the global energy landscape that governs the populations and interconversion rates of conformationally excited states. If these states are thermally accessible (say, within a few k_BT units of the global energy minimum), then the altered topology affects the thermally averaged equilibrium properties of the native state. For instance, disulfide cleavage might allow a loop to fluctuate rapidly among alternative configurations, in which case nuclear Overhauser effects (NOEs) and order parameters, as observed by NMR, would be affected (*29*, *43*).

Because the 14−38 disulfide bond in BPTI is located at the surface, the chemical modifications introduced in BPTI-CS and BPTI-RCAM are not expected to disturb the protein structure significantly. Indeed, IR, ORD, Raman, and NMR spectroscopic studies suggest that the overall solution conformation of BPTI is largely unaffected by reduction (and blocking) of the 14−38 disulfide bond (*17*, *37*−*39*). However, more detailed ^{1}H NMR studies of BPTI-RCAM revealed differences from wild-type BPTI in three-bond scalar couplings (*40*) and chemical shifts (*44*) for residues in the two loops. More recently, large ^{1}H and ^{15}N chemical shift changes near residues 14 and 38 have been reported for BPTI-RM, indicating local structural adaptation (*29*). On the basis of chemical shift changes, early workers concluded that the four internal water molecules in wild-type BPTI are not preserved after cleavage of the 14−38 disulfide bond (*44*). The present MRD study, which monitors these waters molecules directly, demonstrates that they are, in fact, conserved.

Highly excited conformational states, far removed from the ground-state conformation, may be more affected by the altered chain topology. Disulfide cleavage enables large-scale conformational fluctuations that are impossible or imperceptibly slow with an intact disulfide bond. Because highly excited states are sparsely populated, they do not contribute significantly to the equilibrium properties of the native conformational ensemble, such as its (average) structure and binding affinities. However, dynamic processes that involve highly excited states as obligatory intermediates, such as chemical exchange of buried amide hydrogens (*45*) or physical exchange of trapped internal water molecules, may be greatly accelerated by disulfide cleavage.

W122 occupies a small cavity near the 14−38 disulfide bond, with O−S distances of 3.6 and 4.3 Å (*4*). This is one of the most densely packed regions of BPTI with correspondingly low atomic displacement factors (*46*). In fact, no other non-hydrogen atom in BPTI has as many (22) non-hydrogen neighbors within 4 Å as the oxygen atom of W122. Being completely buried, this water molecule cannot exchange with bulk water unless the protein structure undergoes a sizable fluctuation, and because of the dense packing, this is likely to be a highly cooperative fluctuation. The present MRD study shows that the 14−38 disulfide bond, by bridging the two loops, provides an important constraint for exchange of W122. When this bond is broken, the loops have greater conformational freedom and, as a result, the residence time of W122 is drastically reduced, from 170 μs (at 27 °C)

to less than 1 μs. It remains to identify the precise atomic displacements that allow W122 to exchange in wild-type BPTI. The 14−38 disulfide bond can adopt at least three conformations with different χ_1 dihedral angles for C14 and C38 (*6*, *47*−*49*). At room temperature, the mean lifetime of the major conformation with respect to transitions to the minor C14 and C38 rotamers is 30 ms and 1 s, respectively (*49*). Because these transition times are several orders of magnitude longer than the residence time of W122, disulfide isomerization cannot be the rate-limiting step for water exchange.

The exchange of the other three internal water molecules (W111−W113), which are buried between the loops further away from the 14−38 disulfide bond, might also be accelerated by disulfide cleavage, but the MRD data indicate that their residence times remain in the same range, 10^{-8}−10^{-6} s, as for wild-type BPTI. Another indication that disulfide cleavage has little or no effect on the exchange of the three remote internal water molecules comes from a ^{15}N relaxation study, showing that both fast (picosecond to nanosecond) reorientational dynamics of the backbone N−H vectors and slower (microsecond to millisecond) chemical shift modulating conformational fluctuations are virtually unaffected by disulfide cleavage in BPTI-RM (*29*).

Exchange of backbone amide protons requires structural fluctuations that allow water molecules (and OH^- or H_3O^+ ions) to interact directly with the peptide group. Deeply buried amide protons are thought to exchange by a global unfolding mechanism on time scales many orders of magnitude longer than the time scale of internal water exchange (*50*, *51*). However, amide proton exchange in surface-exposed residues is considerably faster and might conceivably involve the same type of localized conformational fluctuations as internal water exchange. Unfortunately, the rates of these conformational fluctuations are not known, since hydrogen exchange experiments in the EX_2 regime only yield the equilibrium protection factor. The amide proton of C14, which is directly hydrogen bonded to W122, has a protection factor of 3700 (*52*). If water exchange and amide proton exchange occur from the same "open" state in a two-state equilibrium, then the residence time of W122 (170 μs at 27 °C) can be identified as the mean lifetime of the "closed" state. By the principle of detailed balance, the mean lifetime of the open state then becomes $170 \times 10^{-6}/3700$ s $\approx$ 50 ns. While this is a reasonable time scale, the two-state model may not be a realistic description of the cooperative atomic displacements involved in the mechanism of water and amide proton exchange from this cavity.

REFERENCES

1. Schellman, J. A. (1955) The stability of hydrogen-bonded peptide structures in aqueous solution, *C. R. Trav. Lab. Carlsberg, Ser. Chim. 29*, 230−259.
2. Goldenberg, D. P. (1992) Native and non-native intermediates in the BPTI folding pathway, *Trends Biochem. Sci. 17*, 257−261.
3. Creighton, T. E. (1997) Protein folding coupled to disulphide bond formation, *Biol. Chem. 378*, 731−744.
4. Wlodawer, A., Walter, J., Huber, R., and Sjölin, L. (1984) Structure of bovine pancreatic trypsin inhibitor. Results of joint neutron and X-ray refinement of crystal form II, *J. Mol. Biol. 180*, 301−329.
5. Vincent, J.-P., and Lazdunski, M. (1972) Trypsin−pancreatic trypsin inhibitor association. Dynamics of the interaction and role of disulfide bridges, *Biochemistry 11*, 2967−2977.
6. Hanson, W. M., Beeser, S. A., Oas, T. G., and Goldenberg, D. P. (2003) Identification of a residue critical for maintaining the functional conformation of BPTI, *J. Mol. Biol. 333*, 425−441.
7. Deisenhofer, J., and Steigemann, W. (1975) Crystallographic refinement of the structure of bovine pancreatic trypsin inhibitor at 1.5 Å resolution, *Acta Crystallogr. B 31*, 238−250.
8. Wlodawer, A., Deisenhofer, J., and Huber, R. (1987) Comparison of two highly refined structures of bovine pancreatic trypsin inhibitor, *J. Mol. Biol. 193*, 145−156.
9. Parkin, S., Rupp, B., and Hope, H. (1996) Structure of bovine pancreatic trypsin inhibitor at 125 K: Definition of carboxyl-terminal residues Glu57 and Ala58, *Acta Crystallogr. D 52*, 18−29.
10. Otting, G., and Wüthrich, K. (1989) Studies of protein hydration in aqueous solution by direct NMR observation of individual protein-bound water molecules, *J. Am. Chem. Soc. 111*, 1871−1875.
11. Denisov, V. P., and Halle, B. (1995) Protein hydration dynamics in aqueous solution: A comparison of bovine pancreatic trypsin inhibitor and ubiquitin by oxygen-17 spin relaxation dispersion, *J. Mol. Biol. 245*, 682−697.
12. Denisov, V. P., Halle, B., Peters, J., and Hörlein, H. D. (1995) Residence times of the buried water molecules in bovine pancreatic trypsin inhibitor and its G36S mutant, *Biochemistry 34*, 9046−9051.
13. Denisov, V. P., Peters, J., Hörlein, H. D., and Halle, B. (1996) Using buried water molecules to explore the energy landscape of proteins, *Nat. Struct. Biol. 3*, 505−509.
14. Kress, L. F., and Laskowski, M. (1967) The basic trypsin inhibitor of bovine pancreas. VII. Reduction with borohydride of disulfide bond linking half-cystine residues 14 and 38, *J. Biol. Chem. 242*, 4925−4929.
15. Creighton, T. E. (1975) Interactions between cysteine residues as probes of protein conformation: The disulphide bond between Cys14 and Cys38 of the pancreatic trypsin inhibitor, *J. Mol. Biol. 96*, 767−776.
16. Kress, L. F., Wilson, K. A., and Laskowski, M. (1968) The basic trypsin inhibitor of bovine pancreas. VIII. Changes in activity following substitution of reduced half-cystine residues 14 and 38 with sulfhydryl reagents, *J. Biol. Chem. 243*, 1758−1762.
17. Vincent, J.-P., Chicheportiche, R., and Lazdunski, M. (1971) The conformational properties of the basic pancreatic trypsin inhibitor, *Eur. J. Biochem. 23*, 401−411.
18. Wagner, G., Stassinopoulou, C. I., and Wüthrich, K. (1984) Amide-proton exchange studies by two-dimensional correlated ^{1}H NMR in two chemically modified analogues of the basic pancreatic trypsin inhibitor, *Eur. J. Biochem. 145*, 431−436.
19. Schwartz, H., Hinz, H.-J., Mehlich, A., Tschesche, H., and Wenzel, H. R. (1987) Stability studies on derivatives of the bovine pancreatic trypsin inhibitor, *Biochemistry 26*, 3544−3551.
20. Hagihara, Y., Shiraki, K., Nakamura, T., Uegaki, K., Takagi, M., Imanaka, T., and Yumoto, N. (2002) Screening for stable mutants with amino acid pairs substituted for the disulfide bond between residues 14 and 38 of bovine pancreatic trypsin inhibitor (BPTI), *J. Biol. Chem. 277*, 51043−51048.
21. Marks, C. B., Naderi, H., Kosen, P. A., Kuntz, I. D., and Anderson, S. (1987) Mutants of bovine pancreatic trypsin inhibitor lacking cysteines 14 and 38 can fold properly, *Science 235*, 1370−1373.
22. Hurle, M. R., Marks, C. B., Kosen, P. A., Anderson, S., and Kuntz, I. D. (1990) Denaturant-dependent folding of bovine pancreatic trypsin inhibitor mutants with two intact disulfide bonds, *Biochemistry 29*, 4410−4419.
23. Naderi, H. M., Thomason, J. F., Borgias, B. A., Anderson, S., James, T. L., and Kuntz, I. D. (1991) ^{1}H NMR assignments and three-dimensional structure of Ala14/Ala38 bovine pancreatic trypsin inhibitor based on two-dimensional NMR and distance geometry, in *Conformations and Forces in Protein Folding* (Nall, B. T., and Dill, K. A., Eds.) pp 86−114, American Asssociation for the Advancement of Science, Washington, DC.
24. Ma, L.-C., and Anderson, S. (1997) Correlation between disulfide reduction and conformational unfolding in bovine pancreatic trypsin inhibitor, *Biochemistry 36*, 3728−3736.
25. Goldenberg, D. P. (1988) Kinetic analysis of the folding and unfolding of a mutant form of bovine pancreatic trypsin inhibitor lacking the cysteine-14 and -38 thiols, *Biochemistry 27*, 2481−2489.
26. Berndt, K. D., Beunink, J., Schröder, W., and Wüthrich, K. (1993) Designed replacement of an internal hydration water molecule in

BPTI: Structural and functional implications of a glycine-to-serine mutation, *Biochemistry 32*, 4564−4570.
27. Denisov, V. P., Venu, K., Peters, J., Hörlein, H. D., and Halle, B. (1997) Orientational disorder and entropy of water in protein cavities, *J. Phys. Chem. B 101*, 9380−9389.
28. Barany, G., Gross, C., Ferrer, M., Barbar, E., Pan, H., and Woodward, C. (1996) Optimized methods for chemical synthesis of bovine pancreatic trypsin inhibitor analogues, in *Techniques in Protein Chemistry* (Marshalk, D., Ed.) Vol. VII, pp 503−514, Academic Press, San Diego.
29. Beeser, S. A., Oas, T. G., and Goldenberg, D. P. (1998) Determinants of backbone dynamics in native BPTI: Cooperative influence of the 14−38 disulfide and the Tyr35 side-chain, *J. Mol. Biol. 284*, 1581−1596.
30. Riddles, P. W., Blakeley, R. L., and Zerner, B. (1983) Reassessment of Ellman reagent, *Methods Enzymol. 91*, 49−60.
31. Denisov, V. P., and Halle, B. (1995) Hydrogen exchange and protein hydration: The deuteron spin relaxation dispersions of bovine pancreatic trypsin inhibitor and ubiquitin, *J. Mol. Biol. 245*, 698−709.
32. Halle, B., Denisov, V. P., and Venu, K. (1999) Multinuclear relaxation dispersion studies of protein hydration, in *Modern Techniques in Protein NMR* (Berliner, L. J., and Krishna, N. R., Eds.) pp 419−484, Plenum, New York.
33. Modig, K., Liepinsh, E., Otting, G., and Halle, B. (2004) Dynamics of protein and peptide hydration, *J. Am. Chem. Soc. 126*, 102−114.
34. Gottschalk, M., Venu, K., and Halle, B. (2003) Protein self-association in solution: The bovine pancreatic trypsin inhibitor decamer, *Biophys. J. 84*, 3941−3958.
35. Hamiaux, C., Prangé, T., Riès-Kautt, M., Ducruix, A., Lafont, S., Astier, J. P., and Veesler, S. (1999) The decameric structure of bovine pancreatic trypsin inhibitor (BPTI) crystallized from thiocyanate at 2.7 Å resolution, *Acta Crystallogr. D 55*, 103−113.
36. Kosen, P. A., Creighton, T. E., and Blout, E. R. (1981) Circular-dichroism spectroscopy of bovine pancreatic trypsin-inhibitor and 5 altered conformational states. Relationship of conformation and the refolding pathway of the trypsin-inhibitor, *Biochemistry 20*, 5744−5754.
37. Wagner, G., Tschesche, H., and Wüthrich, K. (1979) The influence of localized chemical modifications of the basic pancreatic trypsin inhibitor on static and dynamic aspects of the molecular conformation in solution, *Eur. J. Biochem. 95*, 239−248.
38. Brunner, H., Holz, M., and Jering, H. (1974) Raman studies on native, reduced, and modified basic pancreatic trypsin inhibitor, *Eur. J. Biochem. 50*, 129−133.
39. Wagner, G., Kalb, A. J., and Wüthrich, K. (1979) Conformational studies by ^{1}H nuclear magnetic resonance of the basic pancreatic trypsin inhibitor after reduction of the disulfide bond between Cys-14 and Cys-38, *Eur. J. Biochem. 95*, 249−253.
40. Yoshioki, S., Abe, H., Noguti, T., Go, N., and Nagayama, K. (1983) Conformational change of a globular protein elucidated at atomic resolution, *J. Mol. Biol. 170*, 1031−1036.
41. Halle, B. (2004) Protein hydration dynamics in solution: a critical survey, *Philos. Trans. R. Soc. London, Ser. B 359*, 1207−1224.
42. Beeser, S. A., Goldenberg, D. P., and Oas, T. G. (1997) Enhanced protein flexibility caused by a destabilizing amino acid replacement in BPTI, *J. Mol. Biol. 269*, 154−164.
43. Barbar, E., Hare, M., Daragan, V., Barany, G., and Woodward, C. (1998) Dynamics of the conformational ensemble of partially folded bovine pancreatic trypsin inhibitor, *Biochemistry 37*, 7822−7833.
44. Stassinopoulou, C. I., Wagner, G., and Wüthrich, K. (1984) Two-dimensional ^{1}H NMR of two chemically modified analogs of the basic pancreatic trypsin inhibitor, *Eur. J. Biochem. 145*, 423−430.
45. Schulman, B. A., and Kim, P. S. (1994) Hydrogen exchange in BPTI variants that do not share a common disulfide bond, *Protein Sci. 3*, 2226−2232.
46. Halle, B. (2002) Flexibility and packing in proteins, *Proc. Natl. Acad. Sci. U.S.A. 99*, 1274−1279.
47. Szyperski, T., Luginbühl, P., Otting, G., Güntert, P., and Wüthrich, K. (1993) Protein dynamics studied by rotating frame ^{15}N spin relaxation times, *J. Biomol. NMR 3*, 151−164.
48. Otting, G., Liepinsh, E., and Wüthrich, K. (1993) Disulfide bond isomerization in BPTI and BPTI(G36S): An NMR study of correlated mobility in proteins, *Biochemistry 32*, 3571−3582.
49. Grey, M. J., Wang, C., and Palmer, A. G. (2003) Disulfide bond isomerization in basic pancreatic trypsin inhibitor: Multisite chemical exchange quantified by CPMG relaxation dispersion and chemical shift modeling, *J. Am. Chem. Soc. 125*, 14324−14335.
50. Roder, H., Wagner, G., and Wüthrich, K. (1985) Amide proton exchange in proteins by EX_1 kinetics: Studies of the basic pancreatic trypsin inhibitor at variable p^{2}H and temperature, *Biochemistry 24*, 7396−7407.
51. Kim, K.-S., Fuchs, J. A., and Woodward, C. K. (1993) Hydrogen exchange identifies native-state motional domains important in protein folding, *Biochemistry 32*, 9600−9608.
52. Tüchsen, E., Hayes, J. M., Ramaprasad, S., Copie, V., and Woodward, C. (1987) Solvent exchange of buried water and hydrogen exchange of peptide NH groups hydrogen bonded to buried waters in bovine pancreatic trypsin inhibitor, *Biochemistry 26*, 5163−5172.

BI0492049